Eur. Phys. J. A **20**, 443–455 (2004)
DOI 10.1140/epja/i2003-10160-9

THE EUROPEAN PHYSICAL JOURNAL A

Origin of the pseudospin symmetry in the relativistic formalism

S. Marcos[1,a], M. López-Quelle[2], R. Niembro[1], and L.N. Savushkin[3]

[1] Departamento de Física Moderna, Universidad de Cantabria, E-39005 Santander, Spain
[2] Departamento de Física Aplicada, Universidad de Cantabria, E-39005 Santander, Spain
[3] Department of Physics, St. Petersburg University for Telecommunications, 191065 St. Petersburg, Russia

Received: 28 April 2003 / Revised version: 30 October 2003 /
Published online: 18 June 2004 –
Communicated by V. Vento

Abstract. The grounds on which the nuclear pseudospin symmetry (PSS) is supposed to be based are analysed within the relativistic mean-field framework. A connection between the mechanisms responsible for the spin-orbit and pseudospin-orbit splittings is shown. The nature of the PSS is investigated through an extended Dirac equation which allows a generalization of the PSS breaking term. It is shown that the PSS breaking in real nuclei can be explained as a result of a non-perturbative transformation from non-physical solutions of the Dirac equation, which satisfy exactly the PSS, to the physical ones. The PSS breaking term produces important, though qualitatively similar, effects on both states of a pseudospin-orbit doublet. The similarity of these effects increases with the number of nodes of the small component of the Dirac spinor of these states.

PACS. 24.10.Jv Relativistic models – 21.60.Cs Shell model – 21.10.Pc Single-particle levels and strength functions – 24.80.+y Nuclear tests of fundamental interactions and symmetries

1 Introduction

The pseudospin symmetry (PSS) is a symmetry of midweight and heavy nuclei [1–20]. Two single-particle states labelled by "a" and "b" make a pseudospin-orbit doublet (PSD) if their radial–, orbital–, and total–angular-momentum quantum numbers are related by the equations $n_{rb} = n_{ra} - 1$, $l_b = l_a + 2$, and $j_b = j_a + 1 = l_a + 3/2$, respectively. In the limit of exact PSS these two states are degenerate. This symmetry is observed experimentally in both spherical and deformed nuclei and has been introduced in nuclear physics in refs. [1,2]. In the pseudospin formalism, the same pseudo-orbital angular momentum $\tilde{l} = (2j - l)$ is assigned to both states of a PSD.

An essential observation has been made in ref. [5], where the author realized that $\tilde{l}$ is identical to the relativistic quantum number l', *i.e.*, to the orbital angular momentum of the small component $F(r)$ of the nucleon Dirac spinor. In recent years, this observation has motivated an active investigation on the nature of the PSS in the framework of the Dirac phenomenology [6–20].

In the relativistic Hartree formalism, a nucleon in the nucleus is considered as moving in a combination of two very strong fields: an attractive scalar field Σ_S and a repulsive vector field Σ_0 that are almost equal in magnitude, so that one has $|\Sigma_S + \Sigma_0| \ll |\Sigma_S - \Sigma_0|$.

In ref. [5], it has been shown that, in the limit $\Sigma_S + \Sigma_0 = 0$, the PSS becomes exact and, in refs. [10–13], it has been argued that the exact PSS would be realized in the limit of vanishing pseudospin-orbit potential (PSOP). This latter condition is somewhat less restrictive than the first one. Thus, the explanation of the PSS in the framework of the single-particle relativistic models has been based on the two different but related following hypotheses: 1) The magnitude of $\Sigma_S + \Sigma_0$ is small enough to consider the PSS slightly broken in nuclei [5–9]. 2) The PSOP is small enough to justify the approximate PSS observed in PSDs of many nuclei [11–13].

In relation with hypothesis 1), one must be aware that, in the limit $\Sigma_S + \Sigma_0 = 0$, there are no bound states and one could consider as degenerate not only the pseudospin partner states but also many other couples of states. Furthermore, bound and unbound states are very different to consider both type of states to have a similar behaviour in relation with the PSS. Thus, it seems quite risky to base the approximate PSS observed in finite nuclei on the smallness of the quantity $|\Sigma_S + \Sigma_0|$. In fact, as we have shown in ref. [18], this hypothesis is not justified.

In relation with hypothesis 2), we have also shown that, although single-particle bound states do exist in the limit of small PSOP, the PSS obtained in this limit has a mathematical rather than physical character [18], the effect of the PSOP being very strong. In particular, it

[a] e-mail: marcos@unican.es

drastically determines the behaviour of the wave function in the nuclear surface, where the PSOP becomes divergent. Thus, the PSS cannot be justified by the smallness of this potential either.

In refs. [17,20], we have shown for the ^{40}Ca nucleus that the PSS can be understood as the result of a complicated cancellation between different contributions to the single-particle energy of the terms entering the equation for the small component F of the Dirac spinor. The resulting pseudospin-orbit splitting depends on the concrete properties of the single-particle potentials where the nucleons are supposed to move [16–18]. All this shows that the PSS has a dynamical character in the classical sense [21]. We have also pointed out that the exact PSS requires the F wave functions of two pseudospin partners to be somewhat different rather than identical. Also, in ref. [18], we have given a number of arguments explaining the similarity between the two F wave functions belonging to a PSD and have established, at a qualitative level, a connection between the mechanism responsible for the spin-orbit splittings and for the breaking of the PSS. In this work, we shall deepen this mechanism. In ref. [20], we discuss new features that the relativistic Hartree-Fock approach brings about in relation with the PSS.

The aim of this work is: A) to establish a comparison between the mechanisms responsible for the spin-orbit and pseudospin-orbit splittings; B) to determine the influence of the spin-orbit interaction on the PSS; C) to show that the two commonly accepted statements given above and labelled as 1) and 2) fail to describe PSS in finite nuclei. Here, we shall be more precise in some arguments already pointed out in ref. [18]. D) To analyse in detail how the observed PSS can be achieved in atomic nuclei starting from a hypothetical situation of exact PSS.

In sect. 2, we give the basic equations describing the spin-orbit and pseudospin-orbit couplings. In sects. 3 and 4, we study the connection of the PSS with the strength of the spin-orbit interaction and with the magnitude of the $\Sigma_S + \Sigma_0$, respectively. In sect. 5, we investigate the role of the symmetry breaking κ terms in the spin-orbit and pseudospin-orbit schemes. In sect. 6, we provide new arguments to explain the PSS, in particular, to understand the similarity between the F components of the two pseudospin partners. Finally, in sect. 7, we summarize our main results and conclusions.

2 Basic equations for the spin-orbit and pseudospin-orbit couplings

If the radial parts of the upper (big) and lower (small) components of the nucleon Dirac spinor are designated as (G/r) and (F/r), respectively, the Dirac equation for these functions, in the relativistic Hartree approximation (RHA), has the following form (the tensor contribution of the vector mesons being neglected):

$$\begin{aligned} \frac{\mathrm{d}}{\mathrm{d}r}G(r) &= -\tfrac{\kappa}{r}\,G(r) + W\,F(r), \\ \frac{\mathrm{d}}{\mathrm{d}r}F(r) &= V\,G(r) + \tfrac{\kappa}{r}\,F(r). \end{aligned} \tag{1}$$

In this equation, $\kappa \equiv (2j{+}1)(l{-}j) = j(j{+}1){-}\tilde{l}(\tilde{l}{+}1){+}1/4$, whereas

$$V \equiv [\Sigma_S + \Sigma_0 - \epsilon]\,, \qquad W \equiv [2M + \Sigma_S - \Sigma_0 + \epsilon]\,, \tag{2}$$

and ϵ is the single-particle energy (SPE) of a nucleon with bare mass M.

From the Dirac equation (1), one can get the two following equivalent second-order differential equations for the G and F components of the nucleon Dirac spinor:

$$\mathcal{G}_\kappa[G] \equiv -G'' + \left[\frac{W'}{W}\left(\frac{G'}{G} + \frac{\kappa}{r}\right) + \frac{l(l+1)}{r^2} + VW\right]G = 0\,, \tag{3}$$

$$\mathcal{F}_\kappa[F] \equiv -F'' + \left[\frac{V'}{V}\left(\frac{F'}{F} - \frac{\kappa}{r}\right) + \frac{\tilde{l}(\tilde{l}+1)}{r^2} + VW\right]F = 0\,, \tag{4}$$

where the quantity

$$VW = 2MV + 2\epsilon\Sigma_0 + (\Sigma_S^2 - \Sigma_0^2) - \epsilon^2 \tag{5}$$

represents an effective state-dependent potential.

Equations (3) and (4) have the same structure and they look very similar. The main difference between them is that in eq. (3) there appear the terms proportional to W'/W and to $l(l+1)$, whereas in eq. (4) W is replaced by V and l by $\tilde{l}$. Formally, eqs. (3) and (4) establish a strong similarity between the spin-orbit (LS) coupling scheme and the PSS formalism. This similarity calls for studying the relationship between them. In relation with a spin-orbit doublet, we shall say that it exhibits *spin symmetry* if the two states of this doublet have the same energy.

The quantum number κ takes different values for the two states of each spin-orbit and pseudospin-orbit doublet. Thus, in both eqs. (3) and (4) the term proportional to κ explicitly breaks the degeneracy of the two partners of respective doublets. The large spin-orbit splitting observed in many cases in comparison with the small splitting of the PSDs, suggests that the κ term plays a more important role in eq. (3) than in eq. (4). However, as we shall see, *what actually happens is just the opposite.*

Equations (3) and (4) do not have exactly the form of a Schrödinger equation because of the terms containing the first derivatives G' and F', respectively. In eq. (3), the term with G' can be eliminated by making the transformation $\tilde{G} = G \times W^{-1/2}$. The resulting equation for

Table 1. The self-consistent ϵ_i and non–self-consistent ϵ_i^* SPEs of the states corresponding to the neutron PSD in the ^{40}Ca nucleus obtained with the relativistic parameter sets NL-SH [22] and NL3 [23]. The quantities $\epsilon_a - \epsilon_b$ and $\epsilon_a^* - \epsilon_b^*$ represent the splitting of the PSD corresponding to the self-consistent and non–self-consistent calculation, respectively.

Set	**State** (i)	ϵ_i	$\epsilon_a - \epsilon_b$	ϵ_i^*	$\epsilon_a^* - \epsilon_b^*$
NL-SH	$2s_{1/2}$ (a)	-16.17	0.33	-15.09	1.93
	$1d_{3/2}$ (b)	-16.50		-17.02	
NL3	$2s_{1/2}$ (a)	-16.96	-0.79	-15.73	0.65
	$1d_{3/2}$ (b)	-16.17		-16.38	

$\tilde{G}$ exhibits a central and spin-orbit potentials, which are energy dependent. In eq. (4), the corresponding transformation would be $\tilde{F} = F \times V^{-1/2}$. However, for bound states, the potential V becomes zero for some value r_0 of r $[V(r_0) = 0]$ in the nuclear surface and this transformation is not defined at r_0. This fact establishes an essential difference between eqs. (3) and (4) and is a first sign suggesting that the term proportional to V'/V is important in eq. (4).

3 The PSS and the spin-orbit interaction

Connections between the pseudospin symmetry (PSS) and the spin-orbit interaction have been studied in several papers [4,15,18]. As has been discussed in ref. [18], for the states of a pseudospin-orbit doublet (PSD) one has $j_a = l_a + 1/2$, whereas $j_b = l_b - 1/2$. Thus, in a simple shell model approximation, in which the nucleons move in a central and LS potentials, the LS term shifts the single-particle energies (SPEs) ϵ_a and ϵ_b in opposite directions. It means that the splitting of PSDs crucially depends on the strength of the LS interaction. In this non–self-consistent picture, two states of a PSD can be forced to be degenerate if the LS interaction is adequately chosen. However, this degeneracy cannot be reached by choosing the magnitude of $\Sigma_S + \Sigma_0$ and maintaining, at the same time, the nucleus stability. For self-consistent models, the relationship between the LS and pseudo-LS schemes is a bit more complicated than for the simple shell models, due to additional contributions to the LS splittings from other terms in equation for G than the LS term, as a result of the self-consistent procedure.

To be more precise, we have worked out calculations for the ^{40}Ca and ^{208}Pb nuclei within the parameter sets NL-SH [22] and NL3 [23], used in the relativistic mean-field approximation as standard sets. We have focused our attention on the neutron pseudospin-orbit doublets to avoid the effect of the Coulomb interaction, which influences somewhat the proton PSDs. Tables 1 and 2 summarize the corresponding results for the neutron PSDs of the ^{40}Ca and ^{208}Pb nuclei, respectively. The single-particle energies ϵ and ϵ^* represent, in the same order, the self-consistent and non–self-consistent results, being the spin-orbit interaction switched off in the latter case. More precisely, ϵ^* has been obtained by solving the Dirac equation (1) with the self-consistent values of Σ_S and Σ_0 but making arbitrarily $\Sigma_S - \Sigma_0 = 0$ in W. To keep the overall spectra ϵ^* and ϵ with a similar density of levels, we have also contracted the range of Σ_S and Σ_0 in V by making the transformation $r \to 0.8 \times r$. Thus, we can establish a significant dependence of the PSD splittings on the spin-orbit interaction.

Table 2. The same as table 1 but for the ^{208}Pb nucleus and set NL-SH [22].

PSD	**State** (i)	ϵ_i	$\epsilon_a - \epsilon_b$	ϵ_i^*	$\epsilon_a^* - \epsilon_b^*$
1	$2s_{1/2}$ (a)	-41.43	3.23	-41.06	3.83
	$1d_{3/2}$ (b)	-44.66		-44.89	
2	$2p_{3/2}$ (a)	-30.91	4.25	-29.99	5.55
	$1f_{5/2}$ (b)	-35.16		-35.55	
3	$2d_{5/2}$ (a)	-20.62	4.13	-18.88	6.26
	$1g_{7/2}$ (b)	-24.75		-25.14	
4	$3s_{1/2}$ (a)	-17.96	0.91	-17.26	1.62
	$2d_{3/2}$ (b)	-18.87		-18.88	
5	$2f_{7/2}$ (a)	-10.80	3.08	-7.98	5.91
	$1h_{9/2}$ (b)	-13.88		-13.89	
6	$3p_{3/2}$ (a)	-7.85	0.83	-6.25	1.72
	$2f_{5/2}$ (b)	-8.68		-7.98	

Our results for the ^{40}Ca nucleus indicate that the exact PSS needs a bit larger spin-orbit interaction than that obtained in the NL-SH set, whereas the opposite is true in relation with the NL3 set. When the LS interaction is switched off, the PSS is significantly deteriorated for the NL-SH set, whereas for the NL3 set the PSS is satisfied with a similar precision, although the ordering of the pseudospin partners is reversed. Taking into account that the spin-orbit splitting for the $1d$ states is around 7 MeV, one could expect a more drastic breaking of the PSS when the spin-orbit interaction is switched off. If it is not like that it is, in part, because, as the spin-orbit potential is switched off, the modification of the energy of the $1d_{3/2}$ state is very small, in contrast to the stronger modification of the energy of the $1d_{5/2}$ state. The fact that the pseudospin partner of the $1d_{3/2}$ state is an s state, which is not affected by the LS interaction, is also crucial to avoid a stronger degradation of the PSS.

In the ^{208}Pb nucleus, the exact PSS for all neutron PSDs would require a large LS interaction for both the NL-SH and NL3 sets. Thus, when the LS interaction is switched off, the PSS is significantly degraded in all cases[1].

[1] On the contrary, all PSDs would reach a good degree of degeneracy if the LS interaction were increased by about a factor 2 (for example, replacing $\Sigma_S - \Sigma_0$ by $2 \times (\Sigma_S - \Sigma_0)$ in W and r by $1.4 \times r$ to get, on average, a similar single-particle spectrum).

The results discussed in this section show the close relation between the PSS and the strength of the LS interaction, as well as the dynamical character of the PSS (according to the classical interpretation of a dynamical symmetry [21]).

4 The PSS* in finite nuclei and the $\Sigma_S + \Sigma_0$ potential

As is considered in refs. [5–9], the exact PSS with $\epsilon_a = \epsilon_b$ and $F_a = F_b$ can be obtained if $\Sigma_S + \Sigma_0$ is neglected in the V potential in eq. (1). Hereafter, we shall denote this particular type of symmetry by PSS*, and we reserve the notation PSS for the more general case in which only the equality $\epsilon_a = \epsilon_b$ is required. Unfortunately, the condition $\Sigma_S + \Sigma_0 = 0$ is incompatible with real nuclei since it prevents the possibility of bound states.

As we have pointed out in ref. [18], if the reason for the quasi-degeneracy ($\epsilon_a \simeq \epsilon_b$) and similarity of the wave functions ($F_a \simeq F_b$) of both states of a PSD were the small value of $|\Sigma_S + \Sigma_0|$ (as claimed in refs. [5–9]), then, this property should be also exhibited by all PSDs, and the similarity of the wave functions should be regularly intensified as $|\Sigma_S + \Sigma_0|$ decreases ($\Sigma_S - \Sigma_0$ remaining unchanged). However, as we shall see later, this behaviour is not a general rule. Let us analyse first the quasi-degeneracy of the two states of a PSD.

4.1 The condition $\epsilon_a \simeq \epsilon_b$

What one observes when $|\Sigma_S + \Sigma_0|$ decreases is that the binding energy of the states b with $\kappa > 0$ decreases faster than that of their respective pseudospin partners a with $\kappa < 0$ does. Therefore, as long as $\epsilon_b < \epsilon_a$, ϵ_a and ϵ_b approach each other as $|\Sigma_S + \Sigma_0|$ decreases, whereas, when $\epsilon_b > \epsilon_a$, the opposite is true and, in this case, ϵ_a and ϵ_b separate from each other.

To be more precise, we have worked out calculations in which the potential $\Sigma_S + \Sigma_0$ entering V in eq. (2) is considered as a variable quantity. The different values used in the calculations have been obtained from the self-consistent ones by multiplying them by the reduction factor RF. In fig. 1, we have represented, for the ^{40}Ca nucleus, the SPEs of both states of the neutron PSD and their differences as functions of RF. It can be observed that for $\epsilon_b < \epsilon_a$, the quantity $|\epsilon_b - \epsilon_a|$ decreases as the RF factor decreases, but after the crossing point, when $\epsilon_b > \epsilon_a$, $|\epsilon_b - \epsilon_a|$ monotonically increases as RF decreases, even more rapidly than a linear function. Thus, when $\epsilon_b = 0$, ϵ_a is still smaller than -1 MeV. All that happens though, on average, the whole SPE spectrum is compressed as the RF factor is reduced. Similar results can be also found, at a qualitative level, for the NL3 set and for nuclei heavier than the ^{40}Ca one.

The ordering of all PSDs of the ^{208}Pb nucleus with the NL-SH and NL3 sets corresponds to the case $\epsilon_b < \epsilon_a$. Thus, when $|\Sigma_S + \Sigma_0|$ decreases, the energies of the states of a PSD approach each other until they become either

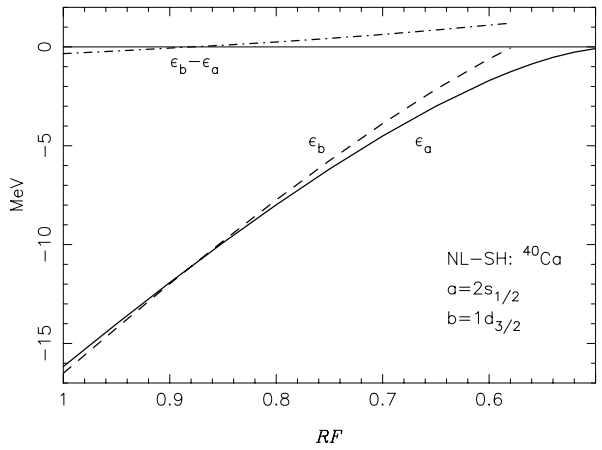

Fig. 1. The SPEs ϵ_a and ϵ_b of the two states $a = 2s_{1/2}$ and $b = 1d_{3/2}$ of the neutron PSD of the ^{40}Ca nucleus and the difference $\epsilon_a - \epsilon_b$ as functions of the reduction factor RF of $\Sigma_S + \Sigma_0$ in the potential V for the NL-SH set [22].

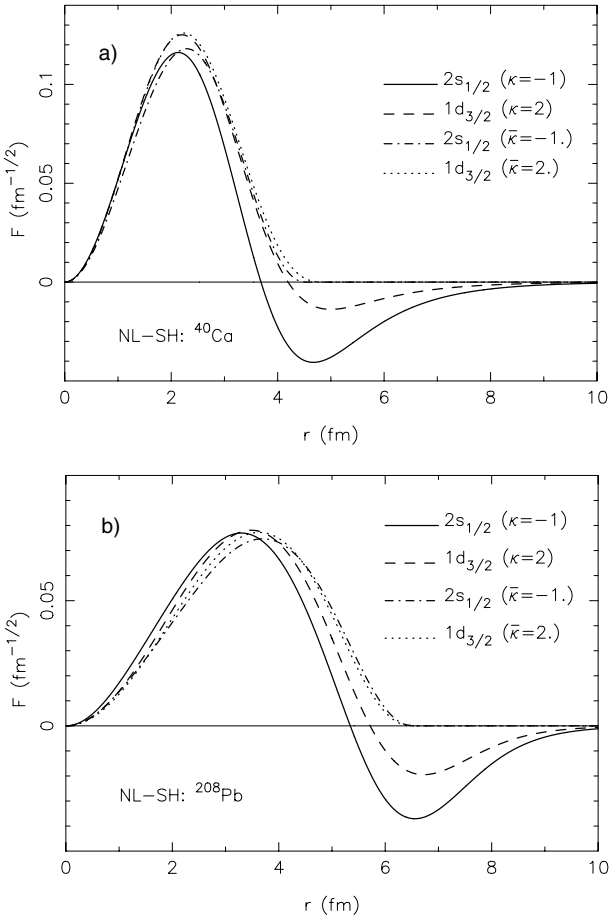

Fig. 2. a) The physical (solid and dashed curves) and the non-physical (dash-dotted and dotted curves) wave functions F for the neutron PSD of the ^{40}Ca nucleus with the NL-SH set. The two non-physical functions F are solutions of eqs. (10) with $\bar{\kappa} \to \kappa_a^-$ and $\bar{\kappa} \to \kappa_b^-$ or with $\bar{\kappa} = \kappa_a$ and $\bar{\kappa} = \kappa_b$ (as the physical states) and the condition $F(r_0) = 0$. b) The same as a) but for the neutron PSD 1 of the ^{208}Pb nucleus.

degenerate or $\epsilon_a = 0$. In the first case, a further reduction of $|\Sigma_S + \Sigma_0|$ produces an increasing of the difference[2] $|\epsilon_b - \epsilon_a|$. This relation between $|\epsilon_b - \epsilon_a|$ and $|\Sigma_S + \Sigma_0|$ also corroborates the dynamical character of the PSS.

These results can be understood by taking into account that the a states with $\kappa < 0$ have larger values of the wave function F in the nuclear surface than the b states with $\kappa > 0$ (see figs. 2a), b), 3a)-c)). *Thus, the decreasing of the quantity $|\Sigma_S + \Sigma_0|$, which takes larger values inside the nucleus than in the surface, affects more the b states than the a ones.*

It is worth recalling that the results just discussed for the nuclear case are quite different from what happens for a relativistic particle moving in two identical potentials Σ_S and Σ_0 of the Coulomb type [5]. In this case, when the magnitude of $|\Sigma_S + \Sigma_0|$ is reduced, the energies of both pseudospin partners increase (become less negative) and always approach each other. This behaviour is due to the fact that, for potentials of Coulomb type, the single-particle level density becomes infinite as the energy ϵ approaches the continuum. Then, as $|\Sigma_S + \Sigma_0|$ decreases, the two states of a PSD remain always bound and r_0, the value of r where the κ term is singular, increases in a similar way for both states. Then, the pseudospin breaking term becomes less important as ϵ approaches the continuum and the energies of the pseudospin partners become closer to each other.

The behaviour of the energy splittings of the pseudospin partners as functions of $|\Sigma_S + \Sigma_0|$ in finite nuclei discussed in this section *is in clear contradiction with what one would expect if the approximate PSS observed in finite nuclei were a consequence of the smallness of the quantity $|\Sigma_S + \Sigma_0|$,* as has been claimed in earlier investigations [5–9] on this subject (see hypothesis 1) in sect. 1).

4.2 The condition $F_a \simeq F_b$

In figs. 2a), b) and 3a)-c), we have represented the small components F of the different neutron PSDs appearing in the ^{40}Ca and ^{208}Pb nuclei. As we have noticed in ref. [18], the main differences between the two components F of a PSD appear for $r \gtrsim r_0$. This fact can be attributed to the divergence at r_0 of the factor V'/V appearing in the PSS breaking term (see the κ term in eq. (4)). In refs. [5–9], the similarity of the two F components of a PSD is also based on the fact that the quantity $|\Sigma_S + \Sigma_0|$ is small (the two conditions $\epsilon_a \simeq \epsilon_b$ and $F_a \simeq F_b$ being closely related). However, *near the singularity point r_0, the ratio V'/V behaves as $(r - r_0)^{-1}$ and shows a weak dependence on $\Sigma_S + \Sigma_0$ only through the value of r_0, which in finite*

[2] In the second case, if the strength of the LS interaction is increased until the two states of the corresponding PSD become degenerate for a given potential $|\Sigma_S + \Sigma_0|$, a further reduction of $|\Sigma_S + \Sigma_0|$ produces also an increasing of $|\epsilon_b - \epsilon_a|$. For example, if we consider the 5th PSD of the ^{208}Pb nucleus, starting from a situation in which $\epsilon_a \simeq \epsilon_b \simeq -10$ MeV and the $|\Sigma_S + \Sigma_0|$ is monotonically reduced, one gets $\epsilon_a < -1$ MeV when $\epsilon_b = 0$.

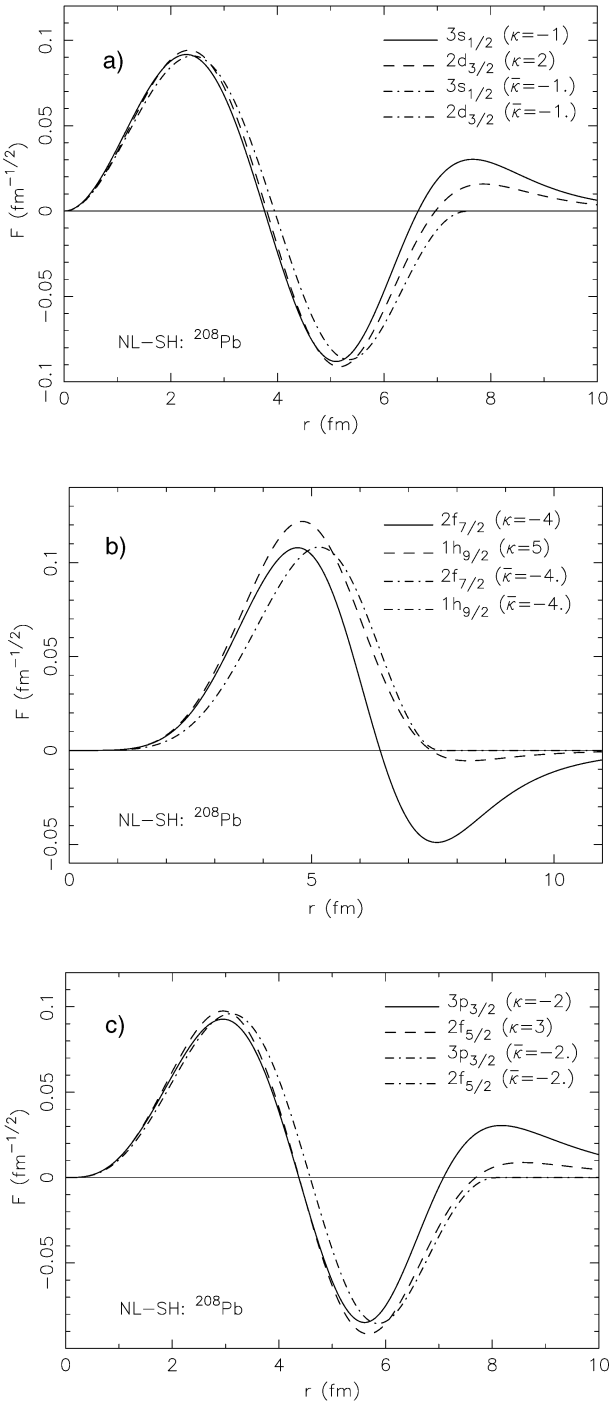

Fig. 3. a) The physical (solid and dashed curves) and the non-physical (dash-dotted curve) wave functions F for the 4th neutron PSD of the ^{208}Pb nucleus with the NL-SH set. The non-physical functions F are solutions of eqs. (10) with $\bar{\kappa} \to \kappa^-$ or with $\bar{\kappa} = \kappa$ (as the physical states) and the condition $F(r_0) = 0$. Notice that, since the $\bar{b}$ and $\bar{a}$ states for the same value of $\bar{\kappa}$ are proportional to each other, the same (dash-dotted) curve can be used to represent $F_{\bar{a}}$ and $F_{\bar{b}}$ although with different norms. In this figure, the state $\bar{b} = 2d_{3/2}$ is not normalized. b) The same as a), but for the neutron PSD 5. c) The same as a), but for the neutron PSD 6.

nuclei lies, in practice, *in a narrow region of about 2 fm in the nuclear surface.* Thus, *the effect of the value of* $\Sigma_S+\Sigma_0$ *in the most important region of the nucleus (around* r_0*) in relation with the condition* $F_a \simeq F_b$*, seems to be quite reduced. All this suggests that the similarity* $F_a \simeq F_b$ *(and, consequently, the PSS*) cannot be justified by the fact that* $|\Sigma_S + \Sigma_0|$ *is small either.*

As we have seen above, in nuclei, contrary to what happens in atoms, the splitting of a PSD does not decrease monotonically as the quantity $|\Sigma_S + \Sigma_0|$ is reduced. Thus, as $|\Sigma_S + \Sigma_0|$ decreases and the binding energy of one of the states of a PSD approaches zero, its corresponding wave function spreads more and more all over the space, whereas that of its partner, which has still a finite binding energy, remains localized. Then, *for two nuclear pseudospin partner states* a *and* b *such that* ϵ_a *or* ϵ_b *is near the continuum, the similarity between* F_a *and* F_b *degrades as* $|\Sigma_S + \Sigma_0|$ *decreases, which seems to be in clear contradiction with the hypothesis that the condition* $F_a \simeq F_b$ *in nuclei is a consequence of the smallness of* $|\Sigma_S + \Sigma_0|$, as is claimed in refs. [5–9].

4.3 Role of the LS interaction in the relationship between the PSS* and the $\Sigma_S + \Sigma_0$ potential

New arguments to support the conclusions made in sects. 4.1 and 4.2 can be found taking into account the effect of the LS interaction on the PSS discussed in sect. 3. To facilitate the comprehension of this point, let us designate those models with realistic values of $\Sigma_S - \Sigma_0$ as models of type I and those with $\Sigma_S - \Sigma_0 = 0$, which means that there is no LS interaction, as models of type II.

The result of exact PSS* obtained in refs. [5–8] for the case $\Sigma_S + \Sigma_0 = 0$ is valid for models of type I as well as for models of type II. However, as we have discussed in sect. 3 (see tables 1 and 2), an adequate spin-orbit interaction is important to get approximate PSS (mainly for the PSD with $\epsilon_a > \epsilon_b$, as it happens in heavy nuclei).

Thus, we have models of type II that, although with $\Sigma_S + \Sigma_0 = 0$ also predict exact PSS*, with realistic values of $\Sigma_S + \Sigma_0$ (as those used to obtain the results denoted with the symbol * in tables 1 and 2) appreciably spoil the PSS in finite nuclei. This shows that the degree of fulfilment of the PSS essentially depends on factors different from the magnitude of $\Sigma_S + \Sigma_0$, in particular, on the strength of the LS interaction.

To see a more drastic effect of the LS interaction on the PSS, instead of switching off the LS interaction, as was made in sect. 3, we could go further and reverse the LS interaction by, for example, making the replacement $(\Sigma_S - \Sigma_0) \to -(\Sigma_S - \Sigma_0)$ in W in eq. (2) (we shall call these models of type III). Thus, the level ordering of a spin-orbit doublet (SOD) would be reversed and the PSS would be degraded even more than in models of type II, although, if we made $\Sigma_S + \Sigma_0 = 0$, we would get also exact PSS* as in models of type I and II.

Actually, for models of type III, if one considers a SOD with the states a, a' and another one with the states b, b', so that the states a and b form a PSD, it will happen, saving exceptions, that $|\epsilon_a - \epsilon_b| > |\epsilon_{a'} - \epsilon_{b'}|$ (see a shell model scheme). Thus, the two states with the closest values of the energies would be no longer those belonging to the same PSD with similar F components, but their respective spin-orbit partners with F components having different number of nodes.

Then, the approximate PSS observed in certain PSDs of some nuclei cannot be explained by the condition that the potential $|\Sigma_S+\Sigma_0|$ is small, because keeping this quantity the same in models of type I, II and III, the degree of validity of the PSS in real nuclei is spoiled progressively and significantly as $\Sigma_S - \Sigma_0$ increases from the negative realistic values in models of type I to the positive unrealistic values in models of type III. All that shows that *the LS interaction plays an essential role in understanding the PSS.* Thus, the magnitude of $\Sigma_S - \Sigma_0$, which determines the spin-orbit interaction in finite nuclei, seems to be much more important in explaining the PSS than the fact that $\Sigma_S \simeq -\Sigma_0$, in clear contradiction with what has been stated in refs. [5–9] and has been commonly accepted by the scientific community.

5 Role of the κ term in eqs. (3) and (4)

The characteristics of the κ term in eqs. (3) and (4), which hereafter we shall refer to as G-κ and F-κ terms, respectively, are determined by the behaviour of the corresponding factors W'/W and V'/V. Whereas W contains the nucleon rest mass and is a large quantity ($W > |\Sigma_S - \Sigma_0|$) everywhere inside the nucleus, V becomes zero for a bound state at $r = r_0$ in the nuclear surface. Thus, W'/W is a finite quantity inside the nucleus, whereas V'/V becomes divergent at r_0. These features of the V and W potentials determine the effects of the G-κ and F-κ terms, respectively, for values of $r \gtrsim r_0$ in the nuclear surface.

It is well known that in the Dirac equation and, consequently, in eqs. (3) and (4) only integer values of κ, both negative (κ_a) and positive (κ_b), have physical meaning. However, from a purely mathematical point of view, one may also consider two equations with the same structure of eqs. (3) and (4) but allowing a continuous variation of the parameter κ (always maintaining the physical values of l and $\tilde{l}$ corresponding to the integer physical κ values). This real parameter will be designated as $\bar{\kappa}$ in what follows. Equations (3) and (4) with κ replaced by $\bar{\kappa}$ can be also obtained from the Dirac equation (1) by replacing V and W by $\bar{V}$ and $\bar{W}$, respectively, defined by the equations

$$\bar{V}(r) = V(r) + \Delta V(r), \quad \Delta V(r) = -\frac{W'}{W^2}\frac{\kappa - \bar{\kappa}}{r}, \qquad (6)$$

$$\bar{W}(r) = W(r) + \Delta W(r), \quad \Delta W(r) = \frac{V'}{V^2}\frac{\kappa - \bar{\kappa}}{r}. \qquad (7)$$

Notice that the replacement $W \to \bar{W}$ is equivalent to the replacement $M \to \bar{M}$, where $\bar{M}$ is defined as

$$\bar{M}(r) = M + \Delta M(r), \quad \Delta M(r) = \frac{V'}{2V^2}\frac{\kappa - \bar{\kappa}}{r}. \qquad (8)$$

The Dirac equation including ΔV reads

$$\frac{\mathrm{d}}{\mathrm{d}r}G(r) = -\frac{\kappa}{r}\,G(r) + W\,F(r),$$

$$\frac{\mathrm{d}}{\mathrm{d}r}F(r) = (V+\Delta V)\,G(r) + \frac{\kappa}{r}\,F(r). \tag{9a}$$

Here, κ can only take the physical integer value κ_a or κ_b, for the state a or b, respectively. The real parameter $\bar{\kappa}$ appears only in ΔV.

The equivalent Schrödinger equation for the G component can be written as

$$\mathcal{G}_{\bar{\kappa}}[G] \equiv -G'' + \left[\frac{W'}{W}\left(\frac{G'}{G} + \frac{\bar{\kappa}}{r}\right) + \frac{l(l+1)}{r^2} + WV\right] G = 0. \tag{9b}$$

The Dirac equation including ΔW reads

$$\frac{\mathrm{d}}{\mathrm{d}r}G(r) = -\frac{\kappa}{r}\,G(r) + (W+\Delta W)\,F(r),$$

$$\frac{\mathrm{d}}{\mathrm{d}r}F(r) = V\,G(r) + \frac{\kappa}{r}\,F(r), \tag{10a}$$

and its equivalent equation for the F component is given by

$$\mathcal{F}_{\bar{\kappa}}[F] \equiv -F'' + \left[\frac{V'}{V}\left(\frac{F'}{F} - \frac{\bar{\kappa}}{r}\right) + \frac{\tilde{l}(\tilde{l}+1)}{r^2} + VW\right] F = 0. \tag{10b}$$

Hereafter, we shall use the labels "$\bar{a}$" and "$\bar{b}$" for the eigenstates of eqs. (9) and (10) with $\kappa = \kappa_a < 0$ and $\kappa = \kappa_b > 0$, respectively. If κ is not specified, it will represent either κ_a or κ_b.

5.1 The G-κ term

The effects of the G-κ term on the G wave function and on its corresponding eigenvalue can be estimated by allowing a free variation of the parameter $\bar{\kappa}$ in eqs. (9). We have worked out calculations for the ^{40}Ca nucleus with the NL-SH set. The results for the neutron SPEs $\epsilon_{\bar{a}}$ and $\epsilon_{\bar{b}}$, with $\bar{a} = 1d_{5/2}$ and $\bar{b} = 1d_{3/2}$, which form a spin-orbit doublet, are represented in fig. 4 as functions of $\bar{\kappa}$. As expected, $\epsilon_{\bar{a}}$ and $\epsilon_{\bar{b}}$ are identical for the same value of $\bar{\kappa}$. They are continuous functions of $\bar{\kappa}$, which cross the physical eigenvalues ϵ_a and ϵ_b (black dots). The effect of the G-$\bar{\kappa}$ term on the SPE is to shift the value of the single-particle energy from $\epsilon_{\bar{a}} = \epsilon_{\bar{b}}$ for $\bar{\kappa} = 0$ to ϵ_a or ϵ_b in a continuous way as $\bar{\kappa}$ varies from $\bar{\kappa} = 0$ to κ_a or κ_b, respectively.

Figure 5 shows the space distribution of the $G_{\bar{a}}$ and $G_{\bar{b}}$ functions. For the same value of $\bar{\kappa}$, they are proportional to each other (rather than identical). They also vary continuously with $\bar{\kappa}$. For $\bar{\kappa} = \kappa$, they coincide with the physical functions: $G_{\bar{a}} = G_a$ and $G_{\bar{b}} = G_b$. For $\kappa = 0$, $G_{\bar{a}}$ and $G_{\bar{b}}$ lie between G_a and G_b. These results mean that *the G-κ (or G-$\bar{\kappa}$) term, though the LS interaction is considered large in nuclear physics, behaves, qualitatively, as a perturbative term.*

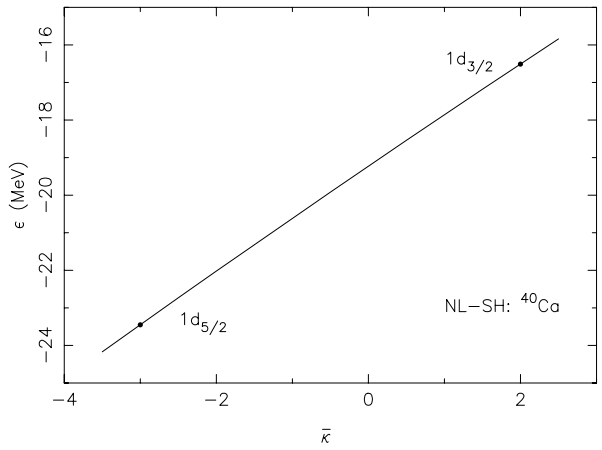

Fig. 4. The SPEs $\epsilon_{\bar{a}}$ and $\epsilon_{\bar{b}}$ as functions of $\bar{\kappa}$, for the $1d$ neutron *spin-orbit doublet* of the ^{40}Ca nucleus and the NL-SH and NL3 sets (the two lines are identical). The dots represent the SPEs corresponding to the physical states.

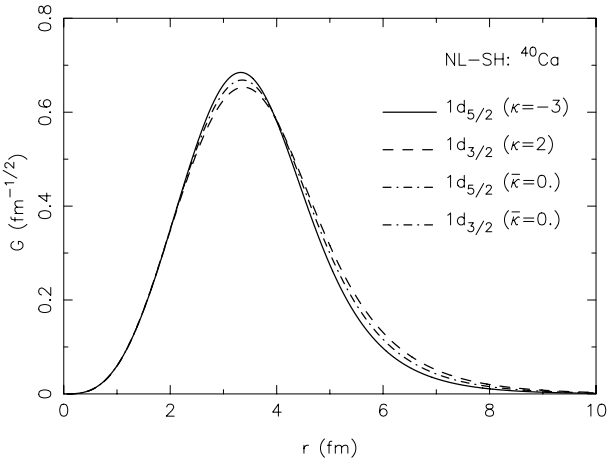

Fig. 5. The $G_{\bar{a}} \equiv G_a$ and $G_{\bar{b}} \equiv G_b$ wave functions, solutions of eqs. (9), with $\bar{\kappa} = \kappa_a$ (or $\bar{\kappa} \to \kappa_a^{\mp}$, solid line) and $\bar{\kappa} = \kappa_b$ (or $\bar{\kappa} \to \kappa_b^{\mp}$, dashed line), respectively, for the $1d$ neutron spin-orbit doublet of the ^{40}Ca nucleus and the NL-SH set. The dash-dotted curve represents the $G_{\bar{a}}$ and $G_{\bar{b}}$ functions for the case $\bar{\kappa} = 0$ (they are proportional to each other, the $1d_{3/2}$ state is not normalized to simplify the figure).

5.2 The F-κ term

To see the effect of the F-κ term in detail, we can proceed as we did to study the effect of the G-κ term on eq. (3). We can solve, now, eqs. (10) for real values of $\bar{\kappa}$. Firstly, one can see quite easily that for $\bar{\kappa} \neq \kappa$ the solutions of eqs. (10) with finite values of $G(r_0)$ and $G'(r_0)$ or $F''(r_0)$ must satisfy the conditions $F'(r_0) = F(r_0) = 0$. This result, by itself, means that *the F-$\bar{\kappa}$ term drastically conditions the behaviour of the F wave function for $r \gtrsim r_0$.* Thus, *this term, as a consequence of its divergence at r_0, plays an essential role in eqs. (10).*

For $\bar{\kappa} = \kappa$, we can find two types of analytic solutions of eqs. (10) quite different: the physical solutions, with normal asymptotic behaviour, and the *non-physical*

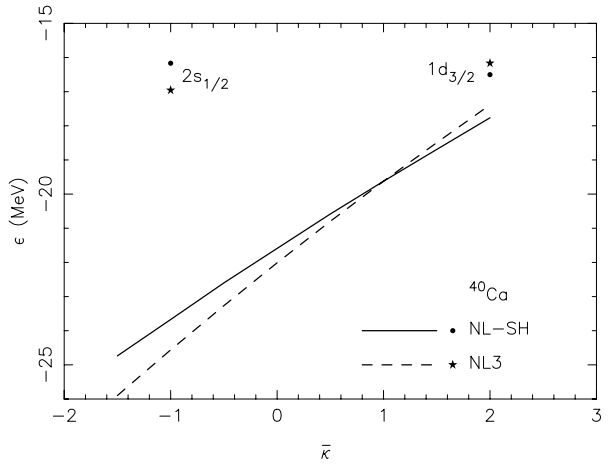

Fig. 6. The *non-physical* SPEs $\epsilon_{\bar{a}}$ and $\epsilon_{\bar{b}}$ as functions of $\bar{\kappa}$, for the neutron PSD of the ^{40}Ca nucleus ($\bar{a} = 2s_{1/2}$ and $\bar{b} = 1d_{3/2}$) and sets NL-SH (solid line) and NL3 (dashed line). The physical SPEs corresponding to the same PSD are also represented for sets NL-SH (dots) and NL3 (stars).

ones, which satisfy the conditions[3] $F'(r_0) = F(r_0) = 0$, and correspond, by continuity, to the solutions obtained in the limit $\bar{\kappa} \to \kappa^-$ (in relation with eqs. (10), we shall use the notation $\bar{a}$ and $\bar{b}$ only for these non-physical solutions). Both types of solutions with $\bar{\kappa} = \kappa_a$ and $\bar{\kappa} = \kappa_b$ are shown in figs. 2a), b) for the neutron PSDs of the ^{40}Ca and ^{208}Pb nuclei, respectively, and the NL-SH set. These figures show that the two physical F wave functions of each PSD are quite similar in the inner region ($r \ll r_0$), whereas they become quite different near the singularity point. As is expected, the difference between the physical and non-physical functions becomes larger for $r \gtrsim r_0$. Similar results are presented for other PSDs of the ^{208}Pb nucleus in figs. 3a)-c).

For real values of $\bar{\kappa} \neq \kappa$, eqs. (9) admit physical and non-physical solutions[4]*, whereas eqs. (10) only admit non-physical solutions due to the singularity of the quantity V^{-1} at r_0. This fact establishes a crucial difference between the role of the G-$\bar{\kappa}$ and F-$\bar{\kappa}$ terms in eqs. (9) and (10), respectively.*

The influence of the F-$\bar{\kappa}$ term on the F function is also reflected in fig. 6, where we have represented the SPE ϵ as a function of $\bar{\kappa}$ for the neutron PSD of the ^{40}Ca nucleus, *i.e.*, for the states $\bar{a} = 2s_{1/2}$ ($\kappa = \kappa_a = -1$) and $\bar{b} = 1d_{3/2}$ ($\kappa = \kappa_b = 2$) and parameter sets NL-SH and NL3. This figure is equivalent to fig. 1 in ref. [18], the numerical uncertainties being minimized. Strictly speaking, the results for both types of solutions (physical and non-physical) discussed in this section are not connected. As we have noticed in ref. [18], the two non-physical states $\bar{a}$ and $\bar{b}$ for the same value of $\bar{\kappa}$ are degenerate. However, we should remind that, for $\bar{\kappa} > \kappa$, ΔW (and $\bar{W}$) becomes a very large negative quantity near r_0 and the Dirac equation cannot properly describe the single-nucleon states. Thus, the degeneracy found for the states $\bar{a}$ and $\bar{b}$ with $\kappa_a < \bar{\kappa}$ is a mathematical rather than a physical result.

If we compare figs. 2a) and 5, we observe that the big components G_a and G_b of the spin-orbit doublet (SOD) of the ^{40}Ca nucleus differ from each other even less than the F_a and F_b components of the PSD do, though the LS splitting is much larger than the pseudospin-orbit splitting. These results also reflect the perturbative character of the G-κ term in eq. (9b) in contrast to the non-perturbative behaviour of the F-κ term in eq. (10b). Actually, because, near the singularity point r_0, $V'/V \sim (r - r_0)^{-1}$, which is an odd function of $r - r_0$, the F-κ term produces a relatively smaller difference between the energies of the two states of a PSD than between their respective wave functions F_a and F_b. This means that the difference of the contributions to the SPE of some terms entering eq. (4), other than the κ term, for both states of a PSD is larger than the splitting of the PSD itself [17,20]. This allows, in particular, the *exact* PSS ($\epsilon_a = \epsilon_b$) to be compatible with $F_a \neq F_b$ [16,17]. *All this suggests that it is more appropriate to associate the pseudospin symmetry to the degeneracy of two states of a PSD than to the similarity of the corresponding F wave functions. For the spin simmetry, however, the two corresponding possibilities are equivalent due to the perturbative character of the symmetry breaking term.*

6 Nature of the PSS

In sect. 5, we have seen that to understand the PSS it is necessary to consider the effect of the F-κ term on the F wave function near the singularity point. For r_0 lying in the nuclear surface, one could expect, in principle, that the effect of this term decreases with the nuclear density at r_0. Thus, for PSDs with values of r_0 such that $\rho(r_0) \ll \rho(0)$ the effect of this term should be small and, consequently, the two states of a PSD should be almost degenerate. In other words, one could expect slightly broken PSS for PSDs with weakly bound states, independently of the values of Σ_S and Σ_0 inside the nucleus. Unfortunately, the best examples of the PSS observed experimentally in nuclei do not correspond to this limiting situation and remain to be explained. Notice that, in nuclear physics, on the contrary to the atomic case, it is not possible, in general, to approach by a continuous reduction of $|\Sigma_S + \Sigma_0|$ both levels of a PSD to the continuum simultaneously (see, for example, fig. 1). This is because the density of the SPE spectrum in nuclear physics remains finite even when ϵ approaches the continuum.

To investigate the origin of the similarity of the small components of the two states of a PSD found in relativistic calculations of finite nuclei, we return to examine the properties of the neutron PSDs of the ^{208}Pb nucleus. The quantum numbers of these states and their corresponding energies obtained for the parameter set NL-SH [22] are

[3] Notice that the condition $F(r_0) = 0$ is artificially imposed in this case (it also leads to $F'(r_0) = 0$), whereas for $\bar{\kappa} \neq \kappa$, necessarily, the condition $F(r \geq r_0) = 0$ has to be satisfied.

[4] With a similar non-standard asymptotic behaviour as the non-physical F functions.

Table 3. Different quantities corresponding to the states of the 6th neutron PSDs of the ^{208}Pb nucleus. The results have been obtained with the relativistic parameter set NL-SH [22]. $\tilde{n}_r$ is the number of nodes of the small component F of the Dirac spinor, $\tilde{l} = 2j - l$ and $\kappa = j(j+1) - \tilde{l}(\tilde{l}+1) + 1/4$. r_{0i} and $r_{0\bar{i}}$ are the values of r such that $V(r) = 0$ in eq. (2) for the *physical* states and for the *non-physical* ones with $\bar{\kappa} = \kappa$, respectively (in the text we have used the same notation r_0 for both r_{0i} and $r_{0\bar{i}}$). $\varepsilon^0_{\bar{i}}(\bar{\kappa})$, $\varepsilon_{\bar{i}}(\bar{\kappa})$, $\varepsilon_{\bar{i}}[\epsilon_{\bar{i}}(\bar{\kappa})]$, and $\varepsilon_{\bar{i}}[\bar{\kappa}, \epsilon_{\bar{i}}(\bar{\kappa})] = \varepsilon_{\bar{i}}(\bar{\kappa}) + \varepsilon_{\bar{i}}[\epsilon_{\bar{i}}(\bar{\kappa})]$, with $i = a, b$, are the contributions to the SPE ϵ_i of the h_0, $-V'/V \times \bar{\kappa}/r$, $2\epsilon\Sigma_0 - \epsilon^2$, and $h(\bar{\kappa}, \epsilon)$ terms in eq. (A.1a), respectively, for the *non-physical* states $F_{\bar{a},\bar{b}}$ calculated for $\bar{\kappa} = \kappa_{a,b}$. Finally, $\Delta\epsilon_i = \epsilon_i - \epsilon_{\bar{i}}(\kappa_i)$, with $i = a, b$, is the sharp energy contribution to the SPE ϵ_i (it represents the energy difference between the physical and non-physical states for $\bar{\kappa} = \kappa$).

PSD	$\tilde{n}_r$	**State** (i)	$\tilde{l}$	$\bar{\kappa} = \kappa_i$	r_{0i}	$r_{0\bar{i}}$	$\varepsilon^0_{\bar{i}}(\bar{\kappa})$	$\varepsilon_{\bar{i}}(\bar{\kappa})$	$\varepsilon_{\bar{i}}[\epsilon_{\bar{i}}]$	$\varepsilon_{\bar{i}}[\bar{\kappa}, \epsilon_{\bar{i}}]$	$\Delta\epsilon_i$	ϵ_i
1	2	$2s_{1/2}$ (a)	1	-1	6.69	6.48	-29.7	0.06	-16.5	-16.4	4.72	-41.42
		$1d_{3/2}$ (b)	1	2	6.54	6.46	-29.7	-0.21	-16.6	-16.8	1.85	-44.67
2	2	$2p_{3/2}$ (a)	2	-2	7.16	6.88	-23.7	-0.27	-13.0	-13.3	6.16	-30.91
		$1f_{5/2}$ (b)	2	3	6.98	6.92	-23.4	0.14	-12.7	-12.8	1.07	-35.16
3	2	$2d_{5/2}$ (a)	3	-3	7.63	7.26	-17.6	-1.14	-9.71	-10.8	7.83	-20.62
		$1g_{7/2}$ (b)	3	4	7.43	7.41	-17.5	0.82	-8.68	-7.86	0.61	-24.75
4	3	$3s_{1/2}$ (a)	1	-1	7.77	7.56	-14.3	-0.44	-7.43	-7.87	4.22	-17.96
		$2d_{3/2}$ (b)	1	2	7.72	7.65	-14.3	0.79	-6.82	-6.03	1.48	-18.87
5	2	$2f_{7/2}$ (a)	4	-4	8.21	7.64	-11.2	-2.55	-6.66	-9.21	9.57	-10.80
		$1h_{9/2}$ (b)	4	5	8.00	7.98	-11.3	1.78	-4.67	-2.89	0.28	-13.88
6	3	$3p_{3/2}$ (a)	2	-2	8.45	8.06	-7.80	-1.00	-4.08	-5.08	5.03	-7.85
		$2f_{5/2}$ (b)	2	3	8.37	8.31	-7.81	1.38	-2.96	-1.58	0.71	-8.68

given[5] in table 3. This table shows that for the PSDs 4 and 6 the PSS is slightly broken. However, for the PSDs 1–3 and 5 the PSS is quite poorly realized. This behaviour seems to be in agreement with the fact that the F wave functions of the PSDs 4 and 6 are much more similar in shape and size than those of the rest of PSDs (see figs. 2b), 3a)-c)). In what follows we shall try to explain these results on other grounds than the smallness of $|\Sigma_S + \Sigma_0|$ in finite nuclei.

6.1 The number of nodes of the G and F functions and the spin and pseudospin symmetries

Table 3 and figs. 2b) and 3a)-c) show that the F wave functions of the PSDs 4 and 6 have 3 nodes, whereas those of the PSDs 1–3 and 5 have only 2 nodes. This difference is an important property that distinguishes both groups of PSDs. Furthermore, for the PSDs 4 and 6, the most relevant part of the F wave functions is developed in a more inner part of the nucleus than for the PSDs 1–3 and 5. This fact suggests that the κ term in eq. (4), which is singular in the nuclear surface, affects the F functions of the PSDs 4 and 6 less than the F functions of the PSDs 1–3 and 5.

A general result, found in all heavy nuclei, is that the degree of similarity between the functions F_a and F_b increases rapidly with the number of their nodes ($\tilde{n}_r$). It seems reasonable to associate this result, mainly, to the increasing with $\tilde{n}_r$ of the local contribution of the term proportional to F'' in eq. (4), which shows the strongest dependence on $\tilde{n}_r$. Thus, the effect of the other terms, including the κ term, becomes relatively less important as F'' gets larger values. The κ term always produces important changes on F (mainly for $r \gtrsim r_0$), however, as $\tilde{n}_r$ increases, its effect on both F_a and F_b functions becomes more similar. This seems to be an essential point to explain the observed similarity between the wave functions F_a and F_b for $\tilde{n}_r \geq 3$ in finite nuclei.

Let us consider now the spin-orbit doublets (SODs). For the two states of a SOD, the degree of similarity of their big components G (so as the degree of degeneracy of their energy levels) also increases rapidly with their number of nodes (n_r) (see figs. 5 and 7a), b)). This effect can be also attributed to a more important role of the term proportional to G'' in eq. (3), in relation with the G-κ term, as n_r increases. However, the G-κ term is almost perturbative, its effect on the G component is much smaller than the effect of the F-κ term on the F component. Thus, for a SOD, there is always a direct correlation between the energy splitting of the two partner states and the similarity of their corresponding G components: the smaller is the splitting the larger is the degree of similarity. For a PSD this correlation fails. In ref. [17], we have shown for the ^{40}Ca nucleus that it is possible to get exact PSS with two quite different functions F_a and F_b. Actually, in real nuclei, the exact PSS, when it happens, can

[5] Similar results are obtained for the NL3 set [23], they will not be reported here.

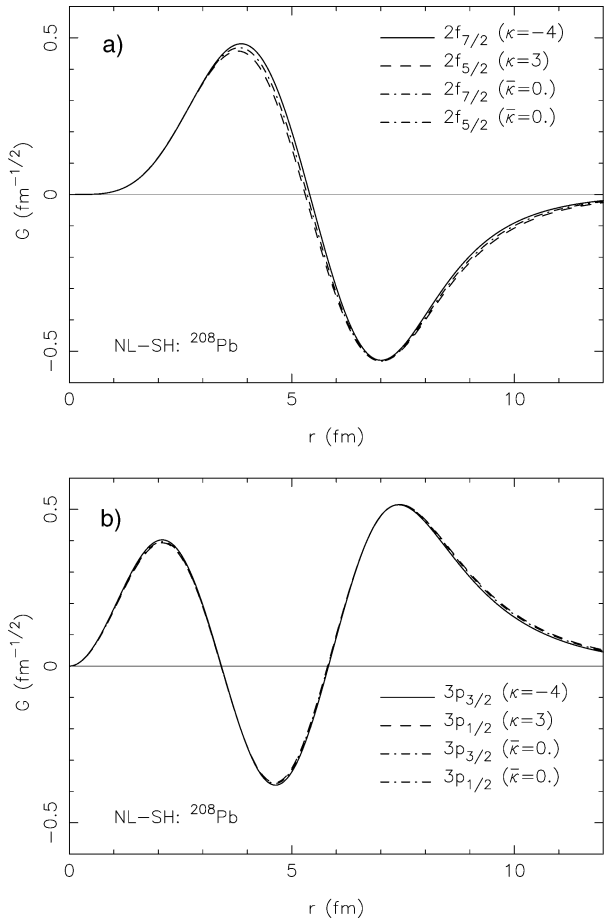

Fig. 7. a) The $G_{\bar{a}} \equiv G_a$ and $G_{\bar{b}} \equiv G_b$ wave functions, solutions of eqs. (9) with $\bar{\kappa} = \kappa_a$ (or $\bar{\kappa} \to \kappa_a^{\mp}$, solid line) and $\bar{\kappa} = \kappa_b$ (or $\bar{\kappa} \to \kappa_b^{\mp}$, dash-dotted line), respectively, for the $2f$ neutron spin-orbit doublet of the ^{208}Pb nucleus and the NL-SH set. The dash-dotted line represents the $G_{\bar{a}}$ and $G_{\bar{b}}$ functions for the case $\bar{\kappa} = 0$ (the $2f_{5/2}$ state is not normalized to simplify the figure). b) The same as a) for the $3p$ neutron spin-orbit doublet.

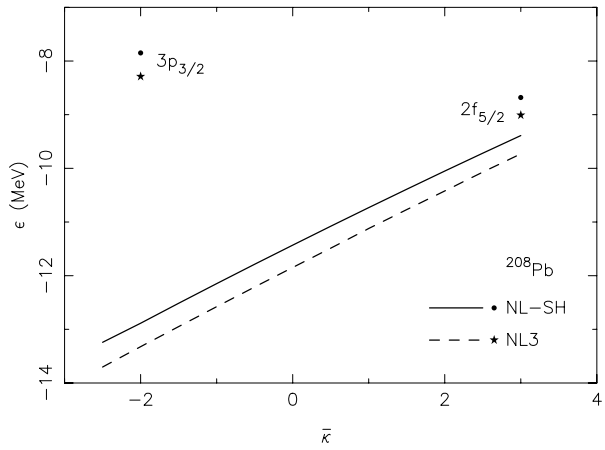

Fig. 8. The non-physical SPEs $\epsilon_{\bar{a}}$ and $\epsilon_{\bar{b}}$ as functions of $\bar{\kappa}$, for the 6th neutron PSD of the ^{208}Pb nucleus ($\bar{a} = 3p_{3/2}$ and $\bar{b} = 2f_{5/2}$) and sets NL-SH (solid line) and NL3 (dashed line). The physical SPEs corresponding to the same PSD are also represented for sets NL-SH (dots) and NL3 (stars).

be only realized with $F_a \neq F_b$. For a SOD, due to the perturbative character of the G-κ term, the exact degeneracy of the two partner states is only possible if the G-κ term itself is switched off.

6.2 Dynamical mechanism of the PSS

To better understand the results discussed for the ^{208}Pb nucleus, we consider again the non-physical solutions of eqs. (10) for the neutron PSDs of this nucleus to find conditions for the exact PSS.

In fig. 8, we have represented the SPEs ϵ corresponding to the two states of the 6th PSD in the ^{208}Pb nucleus, with $\kappa_a = -2$ and $\kappa_b = 3$, as functions of $\bar{\kappa}$. This PSD shows the best realization of the PSS between the PSDs given in tables 2 and 3. As we have explained in sect. 5.2 for the ^{40}Ca nucleus, in this case, for the same value of $\bar{\kappa}$, the states $\bar{a}$ and $\bar{b}$ are always degenerate from the mathematical point of view but, for $\bar{\kappa} > \kappa_a$, this degeneracy cannot be accepted from the physical point of view. In any case, both wave functions $F_{\bar{a}}$ and $F_{\bar{b}}$ are not identical, but only proportional to each other. Thus, *the PSS is exactly and explicitly realizable in some hypothetical nuclear models generating bound states. However, this realization requires, necessarily, the F wave functions to have different norm for the two pseudospin partners.*

In figs. 2a), b), we have drawn, together with the physical functions F_a and F_b, the two corresponding *non-physical* functions $F_{\bar{a}}$ and $F_{\bar{b}}$ (which satisfy the condition $F(r_0) = 0$) for $\bar{\kappa} = \kappa_a$ and $\bar{\kappa} = \kappa_b$, for the ^{40}Ca and ^{208}Pb (PSD 1) nuclei, respectively. It happens that $F_{\bar{b}}$ *remains almost unchanged for all PSDs as $\bar{\kappa}$ varies from κ_a to κ_b. Thus, it can be still appreciated that $F_{\bar{a}}$ (for $\bar{\kappa} = \kappa_a$) and $F_{\bar{b}}$ (for $\bar{\kappa} = \kappa_b$) remain almost proportional to each other.*

Figures 3a)-c) are similar to fig. 2b), but for the PSDs 4–6 of the ^{208}Pb nucleus[6]. For clarity, we have only drawn the *non-physical* function F of the PSD considered corresponding[7] to $\bar{\kappa} = \kappa = \kappa_a < 0$. The function with $\bar{\kappa} = \kappa = \kappa_b > 0$ is very similar to the previous one (as occurs for the PSD 1 in fig. 2b)). Similarly to the ^{40}Ca nucleus, the drastic difference of the energy of the physical and non-physical solutions for $\bar{\kappa} = \kappa$ in the ^{208}Pb nucleus is related with the drastic differences of the corresponding wave functions (see figs. 3c) and 8). These differences are mainly important for $r \gtrsim r_0$. It can be also appreciated that the more relevant part of the physical wave function is shifted through the inner part of the nucleus with respect to the non-physical one.

[6] The results for the PSDs 2 and 3 are quite similar to those for the PSD 5.

[7] The *non-physical* function F with $\bar{\kappa} = \kappa_a$ and $\kappa = \kappa_b > 0$ is exactly proportional to the *non-physical* function F drawn in figs. 3a)-c). Thus, the same function can represent both states although with a different norm. In fig. 3a), for example, the same curve is used for the two non-physical states $3s_{1/2}$ and $2d_{3/2}$ with $\bar{\kappa} = -1$, although the latter state is not normalized.

The main point is that the effect of the κ term, which allows the drastic discontinuous "transition" from the non-physical to the physical F functions, maintains a high degree of similarity between the F functions of the two states of a PSD. Thus, the similarity of $F_{\bar{a}}$ and $F_{\bar{b}}$, for the same value $\bar{\kappa} < \kappa_a$, still remains, at a qualitative level, for the physical functions F_a and F_b. At a quantitative level, however, appreciable differences appear for $r \gtrsim r_0$. In that "transition", the a states with $\kappa < 0$ are more strongly affected than the b states with $\kappa > 0$, since for the former the F function takes larger values in the nuclear surface than for the latter ones. This fact is reflected also in a stronger modification of the SPE of the a states in comparison with that of the b ones, as can be appreciated in figs. 6 and 8.

All these features can be understood by examining carefully eqs. (10). Starting from a physical solution, a small variation of $\bar{\kappa}$, so that $\bar{\kappa} - \kappa \neq 0$ in the effective potential $\Delta W(r)$, produces an important effect on the F wave functions near r_0, where F must become zero. This strong constraint on F at r_0 produces a shift of F through the outer part of the nucleus and explains the difference between the SPEs of the physical and non-physical states: $\Delta\epsilon_{a,b} = \epsilon_{a,b} - \epsilon_{\bar{a},\bar{b}}(\bar{\kappa})$, for $\bar{\kappa} = \kappa_{a,b}$ (or $\bar{\kappa} \to \kappa^{-}_{a,b}$). However, for values of $\bar{\kappa} < \kappa$ the effect of the $\Delta\bar{W}(r)$ term on F is quite independent of the $\bar{\kappa}$ value, only small changes of F with $\bar{\kappa}$ can be appreciated near r_0. *Thus, for $\kappa_a \lesssim \bar{\kappa} \leq \kappa_b$, $F_{\bar{b}}$ remains almost unchanged. In this region, the $\bar{\kappa}$ term is almost perturbative and, consequently, its self-consistent contribution to the SPE of the $\bar{b}$ state is proportional*[8] *to* $\bar{\kappa}$, as can be seen in fig. 8.

As we shall explain in detail in appendix A, in order to get $\epsilon_a \simeq \epsilon_b$ one needs a quasi-compensation between the total contribution of the terms $\bar{\kappa}$, $2\epsilon\Sigma_0$ and ϵ^2 entering eq. (10b) to the SPE of a given non-physical state and the corresponding sharp contribution $\Delta\epsilon$, so that their sum be almost the same for both states a and b (see figs. 6 and 8).

We have discussed in this subsection the dynamical mechanisms allowing a qualitative explanation of the quasi-degeneracy of the two states of a PSD and also the similarity of their respective F wave functions. To understand the different effects of these mechanisms on PSDs of table 3, we have to take into account also the influence of the number of nodes $\tilde{n}_r$ of their F functions. As we have explained in sect. 6.1, *the PSS* is improved as $\tilde{n}_r$ increases.* Thus, table 3 and figs. 2b), 3a)-c) *show that the degeneracy and the proportionality of the F wave functions of the two states of a PSD are improved as $\tilde{n}_r$ increases.* This fact is strongly related with a smaller effect of the F-$\bar{\kappa}$ term on F_a and ϵ_a as $\tilde{n}_r$ increases (see $\Delta\epsilon_a$ in table 3).

From our discussion in sects. 5 and 6, it seems that only if the singularity point r_0 is far enough from the nuclear surface, so that the values $G_i(r_0)$ and $F_i(r_0)$, for $i = a, b$, are small enough, the quasi-equality (or quasi-proportionality) of the F wave functions of the partners of a PSD will only occur. Unfortunately, the states weakly bound (with large values of r_0) have also wave functions with a slow asymptotic decreasing (this effect being more notorious for the state a of a PSD with $\kappa < 0$ than for its partner b[9]). Furthermore, the nuclear force has a small range and $\Sigma_S + \Sigma_0 \to 0$ very fast as $r \to \infty$. Thus, in practice, r_0 is always relatively small, even for states close to the continuum, and the non-physical solutions of eqs. (10) are always significantly different to the physical solutions. These differences affect to a similar extent the inner part of the two physical states of a PSD, but they are much more pronounced for the states a than for the states b for $r \gtrsim r_0$. Thus, in real nuclei, the F wave functions of the two states of a PSD present always appreciable differences for $r \gtrsim r_0$, even for weakly bound states (see figs. 2a), b) and 3a)-c)).

7 Summary and conclusions

The Dirac equation is written in two very similar forms, for both the big G and small F components of the nucleon spinor, where the potentials V and W play, formally, symmetric roles. However, whereas W is always a positive and finite quantity, V becomes zero at the nuclear surface. This fact brings about essential differences between the spin-orbit potential (SOP) and the pseudospin-orbit potential (PSOP). We have shown that, although the SOP is considered to be a big quantity in nuclear physics, it behaves, qualitatively, as a perturbative term. On the contrary, the self-consistent effects of the PSOP, due to the divergence of the factor V^{-1} at the nuclear surface, are very important and the PSOP cannot be treated at all pertubatively.

The relation between the splitting of a PSD and the magnitude of the SOP is analysed in detail. A clear correlation is found between these two magnitudes. For heavy nuclei, a more accurate PSS would require a stronger SOP.

The relation between the PSS and the magnitude of $|\Sigma_S + \Sigma_0|$ is also carefully investigated. It is found that for the PSDs with $\epsilon_a > \epsilon_b$, $|\epsilon_b - \epsilon_a|$ decreases as $|\Sigma_S + \Sigma_0|$ decreases, as is expected. However, for PSDs with $\epsilon_a \leq \epsilon_b$, it happens just the opposite. This result contradicts the interpretation of the PSS as a consequence of the smallness of $|\Sigma_S + \Sigma_0|$ [5–9].

As the number of nodes n_r of the G (or $\tilde{n}_r$ of the F) functions of the two states of a spin-orbit (or pseudospin-orbit) doublet increases, the similarity of these G (or F) functions increases, whereas the splitting of the corresponding doublet decreases. This behaviour is related with a more important role of the terms containing G'' (or F'') in eq. (3) (or eq. (4)), with the increasing of n_r (or $\tilde{n}_r$).

We have shown that the G component in eqs. (9) and, consequently, its corresponding eigenvalue ϵ behave in a *continuous* way as $\bar{\kappa}$ (a real number) varies around the physical value κ. However, the F component in eq. (10) and its corresponding eigenvalue ϵ behave *discontinuously* as $\bar{\kappa}$ varies around the physical value κ. This fact shows the *non-perturbative* character of the F-$\bar{\kappa}$ term in contrast to the *quasi-perturbative* character of the G-$\bar{\kappa}$ term.

[8] Notice that, as the SPE ϵ changes with $\bar{\kappa}$, the contribution to ϵ of the $2\epsilon\Sigma_0$ and ϵ^2 terms, entering eq. (10b) through the quantity VW, also changes, though, because ϵ^2 is very small, ϵ maintains, approximately, its linearity with $\bar{\kappa}$.

[9] It is worth noting that $\Delta\epsilon_i \gg |\epsilon_i|$ as $\epsilon_i \to 0$, for $i = a, b$, but, whereas $\Delta\epsilon_b \to 0$ as $\epsilon_b \to 0$, $\Delta\epsilon_a \not\to 0$ as $\epsilon_a \to 0$.

We have found that for $\bar{\kappa} < \kappa_a$ the PSS is exactly satisfied for (non-physical) "bound" states. Then, allowing $\bar{\kappa}$ to vary from $\bar{\kappa} < \kappa_a$ to κ_a and κ_b, we show how the physical states a and b, and their corresponding eigenvalues, are generated. This enables us to understand the similarity between the small components of the two states of some PSDs and their approximate degeneracy. This degeneracy can be explained as the result of a partial compensation between different contributions, perturbative and non-perturbative, to the SPE, as the nucleus goes from the non-physical satates (with $\bar{\kappa} < \kappa_a$) to the physical ones, showing the dynamical character of the PSS.

We are thankful to V.N. Fomenko for useful discussions. One of us (L.N.S.) is grateful to the University of Cantabria for hospitality. This work has been supported by the DGESIC grand BFM2001-1243.

Appendix A. Quantitative analysis of the relation $\epsilon_a \simeq \epsilon_b$ for the SPEs of a PSD

To better understand how the quasi-degeneracy of the two partners of a PSD is achieved (see figs. 6 and 8), let us write eq. (10b) as

$$[h_0 + h(\bar{\kappa}, \epsilon)]F = \epsilon F, \tag{A.1a}$$

where h_0 depends neither on $\bar{\kappa}$ nor on ϵ, and

$$h(\bar{\kappa}, \epsilon) = -\frac{V'}{V}\frac{\bar{\kappa}}{r} + 2\epsilon\Sigma_0 - \epsilon^2. \tag{A.1b}$$

If we consider the *non-physical* $F_{\bar{i}}$ function normalized to the unity, $\langle F_{\bar{i}}|F_{\bar{i}}\rangle = 1$, for $\bar{i} = \bar{a}, \bar{b}$ and a given value of $\bar{\kappa}$, the contributions of h_0 and $h(\bar{\kappa}, \epsilon)$ to the SPE $[\epsilon_{\bar{i}}(\bar{\kappa})]$ are given by $\varepsilon^0_{\bar{i}}(\bar{\kappa}) = \langle F_{\bar{i}}|h_0|F_{\bar{i}}\rangle$ and $\varepsilon_{\bar{i}}[\bar{\kappa}, \epsilon] = \langle F_{\bar{i}}|h(\bar{\kappa}, \epsilon)|F_{\bar{i}}\rangle$, respectively. We have explained in sect. 6.2 that $F_{\bar{b}}$ remains almost unchanged as $\bar{\kappa}$ varies from κ_a to κ_b. Then, in the interval $\kappa_a \lesssim \bar{\kappa} \leq \kappa_b$, $\varepsilon^0_{\bar{b}}(\bar{\kappa})$ is almost constant and $\varepsilon_{\bar{b}}[\bar{\kappa}, \epsilon]$ can be calculated approximately in a perturbative way (*i.e.*, with the $F_{\bar{b}}$ corresponding to any value of $\bar{\kappa}$ in that interval). These facts explain the linearity of $\epsilon_{\bar{b}}$ as a function of $\bar{\kappa}$ observed in figs. 6 and 8.

We write the SPE for the i physical state as

$$\begin{aligned} &\epsilon_i = \epsilon_{\bar{i}}(\bar{\kappa}) + \Delta\epsilon_i, \qquad && \epsilon_{\bar{i}}(\bar{\kappa}) = \varepsilon^0_{\bar{i}}(\bar{\kappa}) + \varepsilon_{\bar{i}}[\bar{\kappa}, \epsilon_{\bar{i}}(\bar{\kappa})], \\ &\bar{\kappa} = \kappa_i, && i = a, b, \end{aligned} \tag{A.2}$$

where $\epsilon_{\bar{i}}(\bar{\kappa})$ represents the SPE of the $\bar{i}$ *non-physical* state corresponding to $\bar{\kappa} = \kappa_i$ (or $\bar{\kappa} \to \kappa_i^-$) and $\Delta\epsilon_i$ is defined by this equation.

Taking into account that for $\bar{\kappa} < \kappa_a$, $F_{\bar{b}}$ is proportional to $F_{\bar{a}}$ (and consequently $\epsilon_{\bar{b}}(\bar{\kappa}) = \epsilon_{\bar{a}}(\bar{\kappa})$) and that for $\bar{\kappa} \leq \kappa_b$ the effect of the $\bar{\kappa}$ term on the *non-physical* $\bar{b}$ state can be considered, approximately, as perturbative (*i.e.*, $F_{\bar{b}}$ remains almost independent of $\bar{\kappa}$), we can conclude that $\varepsilon^0_{\bar{a}}(\kappa_a) \simeq \varepsilon^0_{\bar{b}}(\kappa_b)$. This approximation can be checked using the results given in table 3 for the ^{208}Pb nucleus. The small difference between these two energies is only due to the small difference between $F_{\bar{b}}$ (for $\bar{\kappa} = \kappa_a$) and $F_{\bar{b}}$ (for $\bar{\kappa} = \kappa_b$). If only perturbative effects were considered, the difference of energy of the two *physical* states of a PSD would be given approximately by the difference $\varepsilon_{\bar{a}}[\kappa_a, \epsilon_{\bar{a}}(\kappa_a)] - \varepsilon_{\bar{b}}[\kappa_b, \epsilon_{\bar{b}}(\kappa_b)]$. The results from table 3 show that, for the PSDs 4–6, $|\varepsilon_{\bar{a}}[\kappa_a, \epsilon_{\bar{a}}(\kappa_a)] - \varepsilon_{\bar{b}}[\kappa_b, \epsilon_{\bar{b}}(\kappa_b)]|$ is larger than $|\epsilon_a - \epsilon_b|$ and, what is more surprising, the energy differences, themselves, have opposite signs for all PSDs except for the first one. All that points out that the origin of the PSS cannot be attributed to the smallness of the κ term.

Since $V(r) < 0$ for $r < r_0$, $V' > 0$ in the nuclear surface and $F_{\bar{a},\bar{b}}(r) = 0$ for $r \gtrsim r_0$, we can expect $\langle F_{\bar{a},\bar{b}}| - V'/V \times 1/r|F_{\bar{a},\bar{b}}\rangle > 0$, at least for the less bound states for which r_0 is larger (and V' remains positive[10] in the region where V^{-1} is big). This is just what happens in the ^{208}Pb nucleus, where only for the first PSD the mean value is negative (see values of $\varepsilon(\bar{\kappa})$ in table 3). Then, we should have $\varepsilon_{\bar{a}}[\kappa_a, \epsilon_{\bar{a}}(\kappa_a)] < \varepsilon_{\bar{b}}[\kappa_b, \epsilon_{\bar{b}}(\kappa_b)]$, at least for the states closest to the Fermi level, as the results of table 3 show for the quantity $\varepsilon_{\bar{i}}[\bar{\kappa}, \epsilon_{\bar{i}}]$, $\bar{i} = \bar{a}, \bar{b}$.

Then, since $\varepsilon^0_{\bar{a}}(\kappa_a) \simeq \varepsilon^0_{\bar{b}}(\kappa_b)$, from eq. (A.2) one can see that to get an approximate PSS for a PSD in real nuclei, it is necessary the sharp contribution $\Delta\epsilon$ to the SPE to be larger for the a state than for the b one: $\Delta\epsilon_a > \Delta\epsilon_b$.

The effects of $\Delta W(r)$ on the SPE ϵ when going from the physical to the non-physical wave function are more pronounced for the states a with $\kappa < 0$ (than for the states b with $\kappa > 0$), because their F and G components take more significant values for $r \gtrsim r_0$ (notice that the G component of these states of PSDs has one node more than that of the states with $\kappa > 0$ and their outer maximum is closer to the singularity point). The larger effect produced by $\Delta W(r)$ for $\bar{\kappa} \neq \kappa$ on the a states than on the b ones is also reflected in the inequality: $\Delta\epsilon_a > \Delta\epsilon_b$. Thus, the PSS, when it occurs, is realized because the Dirac equation generates dynamically the approximation

$$\varepsilon_{\bar{a}}[\kappa_a, \epsilon_{\bar{a}}(\kappa_a)] + \Delta\epsilon_a \simeq \varepsilon_{\bar{b}}[\kappa_b, \epsilon_{\bar{b}}(\kappa_b)] + \Delta\epsilon_b, \tag{A.3}$$

which explains the quasi-degeneracy of many pseudospin partners in finite nuclei[11].

Since $\Delta\epsilon_a > \Delta\epsilon_b$ seems to be a common rule and the inequality $\varepsilon[\kappa_a, \epsilon_{\bar{a}}(\kappa_a)] < \varepsilon[\kappa_b, \epsilon_{\bar{b}}(\kappa_b)]$ occurs, at least, for the states of the PSDs closest to the Fermi surface, it means that for these states there is a kind of compensation between the contributions to the SPE of the two terms involved in these inequalities, which is responsible for a small splitting of these PSDs.

The quasi-degeneracy of a PSD, when it happens, cannot be explained only as a result of the similarity of the two corresponding F wave functions. One should be aware

[10] Notice that, generally, V is not a monotonically increasing function of r (except in the nuclear surface).

[11] Considering only the "perturbative contribution" $\varepsilon_{\bar{i}}[\kappa_i, \epsilon_{\bar{i}}(\kappa_i)]$ of $h(\kappa, \epsilon)$ to the SPE ϵ_i, the splitting of the PSDs in table 3, except for the first PSD, would exhibit a sign opposite to the one obtained when all contributions are included.

that for two identical F wave functions the energy of the two states of a PSD would differ, approximately, by the quantity $\varepsilon_{\bar{a}}[\kappa_a, \epsilon_{\bar{a}}(\kappa_a)] - \varepsilon_{\bar{b}}[\kappa_b, \epsilon_{\bar{b}}(\kappa_b)]$ which, in some of the examples shown in table 3, is quite large and, with the only exception of the first PSD, has the opposite sign to the quantity $\epsilon_a - \epsilon_b$. Then, to get almost exact PSS under these circumstances, the F_a and F_b wave functions must differ from each other in such a way that the quantities $\Delta\epsilon_a$ and $\Delta\epsilon_b$, together with $\varepsilon_{\bar{a}}[\kappa_a, \epsilon_{\bar{a}}]$ and $\varepsilon_{\bar{b}}[\kappa_b, \epsilon_{\bar{b}}]$, could satisfy eq. (A.3). The difference between F_a and F_b that is necessary to get approximate PSS decreases with the increasing of their number of nodes.

In the ^{208}Pb nucleus, the F wave functions of the 6th PSD, which is considered as one of the best examples of PSS, exhibit clear differences for large values of r (see fig. 3c)). The almost exact degeneracy of the $3p_{3/2}$ and $2f_{5/2}$ states (see table 3) cannot be explained due to the smallness of the κ term (as a consequence of the validity of the $(\Sigma_S + \Sigma_0 = 0)$-limit) but, rather, due to the fact that F_a and F_b differ from each other just enough to generate differences between $\Delta\epsilon_a$ and $\Delta\epsilon_b$ so that eq. (A.3) is approximately satisfied. In refs. [17,20], one can see more details of the complicated cancellation of the contributions to the single-particle energies of the different terms entering eq. (4) that, in particular, allows the quasi-degeneracy of the $3p_{3/2}$ and $2f_{5/2}$ states. It is also shown that this cancellation, by itself, can explain the approximate degeneracy observed in the PSDs of the nuclei for which the functions F_a and F_b, with a number of nodes $\tilde{n} = 2$, differ from each other appreciably.

When F_a and F_b differ more (or less) than it is necessary to satisfy eq. (A.3), the PSS is not well realized. This is just what happens, for example, with the states of the PSDs 1–3 and 5 of the ^{208}Pb nucleus.

References

1. A. Arima, M. Harvey, K. Shimizu, Phys. Lett. B **30**, 517 (1969).
2. K.T. Hecht, A. Adler, Nucl. Phys. A **137**, 129 (1969).
3. C. Bahri, J.P. Draayer, S.A. Moszkowski, Phys. Rev. Lett. **68**, 2133 (1992).
4. A.L. Blokhin, C. Bahri, J.P. Draayer, Phys. Rev. Lett. **74**, 4149 (1995).
5. J.N. Ginocchio, Phys. Rev. Lett. **78**, 436 (1997); Phys. Rep. **315**, 231 (1999).
6. J.N. Ginocchio, D.G. Madland, Phys. Rev. C **57**, 1167 (1998).
7. J.N. Ginocchio, J. Phys. G **25**, 617 (1999).
8. J.N. Ginocchio, Phys. Rep. **315**, 231 (1999).
9. J.N. Ginocchio, A. Leviatan, Phys. Rev. Lett. **87**, 072502 (2001).
10. K. Sugawara-Tanabe, A. Arima, Phys. Rev. C **58**, R3065 (1998).
11. J. Meng, K. Sugawara-Tanabe, S. Yamaji, P. Ring, A. Arima, Phys. Rev. C **58**, R628 (1998).
12. J. Meng, K. Sugawara-Tanabe, S. Yamaji, A. Arima, Phys. Rev. C **59**, 154 (1999).
13. K. Sugawara-Tanabe, J. Meng, S. Yamaji, A. Arima, J. Phys. G **25**, 811 (1999).
14. P. Ring, J. Phys. G **25**, 641 (1999).
15. Y.K. Gambhir, J.P. Maharana, C.S. Warke, Eur. Phys. J. A **3**, 255 (1998).
16. S. Marcos, L.N. Savushkin, M. López-Quelle, P. Ring, Phys. Rev. C **62**, 054309 (2000).
17. S. Marcos, M. López-Quelle, R. Niembro, L.N. Savushkin, P. Bernardos, Phys. Lett. B **513**, 30 (2001).
18. S. Marcos, M. López-Quelle, R. Niembro, L.N. Savushkin, P. Bernardos, Eur. Phys. J. A **17**, 173 (2003).
19. P. Alberto, M. Fiolhais, M. Malheiro, A. Delfino, M. Chiapparini, Phys. Rev. Lett. **86**, 5015 (2001); Phys. Rev. C **65**, 034307 (2002); R. Lisboa, M. Malheiro, P. Alberto, Phys. Rev. C **67**, 054305 (2003).
20. M. López-Quelle, L.N. Savushkin, S. Marcos, P. Bernardos, R. Niembro, to be published in Nucl. Phys. A.
21. G.F. Torres, J.L. Calvario, Rev. Mex. Fis. **43**, 649 (1997); A. Arima, *Dynamical Symmetries and Nuclear Structure*, preprint RIKEN-AF-NP-276.
22. M.M. Sharma, M.A. Nagarajan, P. Ring, Phys. Lett. B **312**, 377 (1993).
23. G.A. Lalazissis, J. König, P. Ring, Phys. Rev. C **55**, 540 (1997).